Buckling of Imperfect Elliptical Cylindrical Shells under Axial Compression

R. C. TENNYSON,* M. BOOTON,† AND R. D. CASWELL†
University of Toronto Institute for Aerospace Studies, Toronto, Ontario, Canada

Results have been obtained for a wide range of cylinder eccentricities ($0.5 \leq B/A \leq 1.0$) which clearly demonstrate that elliptical shells are imperfection sensitive. Elliptical cylinders containing axial imperfection distributions of various wavelengths were subjected to axial compression and their buckling loads compared with those obtained from a corresponding set of geometrically "near-perfect" elliptical cylinders. The shells were sufficiently thin to employ the circular cylinder approximation based on the curvature at the ends of the minor axis to calculate buckling loads. For the case of the perfect elliptical cylinders, theory and experiment were in close agreement. In addition, significant load reductions were found for the imperfect shells for small values of the imperfection amplitude, consistent with predictions based on an equivalent axisymmetric imperfect circular cylinder theory. It was also observed that a critical axial imperfection wavelength existed which resulted in a minimum buckling load. Postbuckling behaviour was also investigated to determine the extent to which the maximum compressive loads exceeded the initial buckling value as a function of cylinder eccentricity.

Nomenclature

A = length of semimajor axis
B = length of semiminor axis
b = postbuckling coefficient
c = $[3(1 - \nu^2)]^{1/2}$
e = $[1 - (B/A)^2]^{1/2}$
E = modulus of elasticity
K = p/q_o
L = shell length
lx = $L/M = \pi R_B/2p$, axial half-wavelength
M,N = number of half waves and waves in the axial and circumferential directions, respectively
p = $M\pi R_B/2L$
q_o = $(R_B/t)^{1/2}[12(1 - \nu^2)]^{1/4}$, the equivalent circular cylinder classical axisymmetric buckling mode wave number
R_B = A^2/B, radius of curvature of elliptical cylinder at ends of minor axis
R_o = perimeter length$/2\pi$
R_s = $A^2/B\{1 + [(B/A)^2 - 1](Y/A)^2\}^{3/2}$, radius of curvature of ellipse
s = circumferential coordinate
t = shell wall thickness
$\bar{t}$ = average shell wall thickness
w = outward normal displacement
$\bar{w}$ = initial outward normal displacement of median surface
$\tilde{W}$ = $\bar{w}/t$
X,Y,Z = Cartesian coordinates (Fig. 1)
δ = peak axial imperfection amplitude
ϵ = applied compressive strain
λ = buckling load of imperfect shell/buckling load of perfect shell
λ_K = theoretical value of λ derived from Koiter's axisymmetric imperfect circular cylinder theory [Eq. (6)]
μ = maximum deviation of median surface/average shell wall thickness
ν = Poisson's ratio
σ = applied compressive stress
σ_{c_c} = Et/R_oc, classical buckling stress for circular cylinder of radius R_o
σ_{C_E} = Et/R_Bc, approximate buckling stress of elliptical cylinder
$\sigma_{cr},\sigma_{cr}^*$ = experimental buckling stress of perfect and imperfect cylinders, respectively
$\sigma_{\max},\sigma_{\max}^*$ = maximum experimental compressive stress of perfect and imperfect cylinders, respectively
τ = $N(t/R_Bc)^{1/2}$

Received May 22, 1970; revision received August 20, 1970. The authors wish to gratefully acknowledge the financial assistance of the National Research Council of Canada (Grant A-2783) and of the NASA [Grant NGR 52-026-(011), Supplement No. 2] which made this research possible.

* Associate Professor. Member AIAA.
† Research Assistant.

I. Introduction

THE buckling and postbuckling behaviour of oval cylindrical shells subjected to axial compression has been studied only recently.[1-4] Although considerable attention has been given to determining the effect of initial shape imperfections on the buckling of circular cylinders, only one theoretical analysis of the imperfection sensitivity of oval cylinders as a function of shell eccentricity exists.[3] Initial studies made by Kempner and Chen[1,2,4] indicated that oval cylinders with moderate to high eccentricity ($B/A \leq 0.7$) appeared to demonstrate little or no sensitivity to shape imperfections based on their buckling and postbuckling results. However, Hutchinson[3] has shown theoretically that significant imperfection sensitivity exists for the range of $B/A \geq 0.2$ providing $R_o/t \geq 200$. Subsequently, Kempner and Chen[4] confirmed that initial snap-through buckling action was possible for oval cylinders, although the extent to which it would be noticeable for highly eccentric shells might be negligible. It is generally agreed that for values of B/A close to unity, the oval cylinder behaviour should closely approximate that of a circular shell. It thus remains to determine the transition region between circular cylinder and flat plate buckling behaviour in terms of imperfection sensitivity. From a design point of view, it is imperative to know the extent to which an oval cylinder is sensitive to shape imperfection distributions, since it is well known that small amplitude deviations from the perfect shell configuration result in drastic load reductions below the classical value for circular cylinders.[5]

Although some experimental buckling data has been accumulated on oval cylinders subjected to axial compression,[2-4] insufficient results exist over a wide range of the eccentricity parameter (B/A) to verify the perfect shell theory. What has consistently emerged from all test data

to date, however, is the fact that for certain values of eccentricity, postbuckling loads in excess of the initial buckling load can be obtained, as predicted by Kempner and Chen.[2,4] Consequently for this class of oval shells, it has been proposed that the higher postbuckling loads be used for design purposes, since they characterize a total collapse mode similar to the circular cylinder. The major difficulty with this approach is the extensive plastic deformation in the vicinity of the buckle nodes which propagates circumferentially as the applied load is increased above the initial buckling value for metal cylinders. Hence, it is of primary importance to determine the initial buckling load for oval cylinders and the extent to which it is affected by geometrical shape imperfections. As a result, it was decided to investigate the axial compressive buckling behaviour of a series of elliptical thin-walled cylinders containing a specific shape imperfection having the form of a simple sine wave which was a function only of the axial coordinate. The technique employed[5] to fabricate the imperfection distribution resulted in an axial thickness variation, since the profile was cut on the inner shell wall surface only. However, it has been shown[5] that the effect of the variable thickness is small, and the dominant factor in reducing the cylinder buckling loads is the shape imperfection associated with the deviation of the median surface. In order to assess the degree of degradation in the buckling load for a wide range of eccentricities ($0.5 \leq B/A \leq 1.0$), an additional set of elliptical cylinders having no prescribed shape imperfections was tested in axial compression to serve as reference data for a class of geometrically near-perfect shells. This latter test series provided a measure of the load reduction due to the manufacturing process and the clamped-edge constraints. It was also of particular interest to determine if the critical buckling load could be accurately predicted, based on circular cylinder theory using the local radius of curvature at the minor axis. This approximation also permitted a comparison of the experimental buckling loads for the elliptical cylinders having an axial imperfection distribution with the analytical results obtained for equivalent axisymmetric imperfect circular cylinders.[5]

II. Basic Equations

In general, for an oval cylinder, buckling initiates in the region of minimum curvature defined by the minor axis (Fig. 1). It has been shown that for a sufficiently thin-walled oval shell, the buckling stress can be approximated by the classical circular cylinder equation[1,3]

$$\sigma_{c_E} = Et/R_B c \tag{1}$$

where R_B is the local radius of curvature at the ends of the minor axis. For the case of an elliptical cross section, $R_B = A^2/B$. The effect of cylinder ellipticity on reducing the initial buckling load below the equivalent circular cylinder value can be determined from the relationship

$$\sigma_{c_E}/\sigma_{c_C} = R_o/R_B \tag{2}$$

where R_o = perimeter length/2π

$$= \frac{2A}{\pi}\int_0^{\pi/2}(1 - e^2\sin^2\theta)^{1/2}d\theta \tag{3}$$

Hutchinson[3] has shown that for

$$[12(1 - \nu^2)]^{1/2}R_o/t \geq 625 \tag{4}$$

the critical buckling load for an elliptical cylinder differs from the value given by Eq. (1) by less than 5% for $B/A \geq 0.20$. Thus, for the range of elliptical shells considered in this investigation, Eq. (1) will be used to predict the "perfect shell" buckling loads.

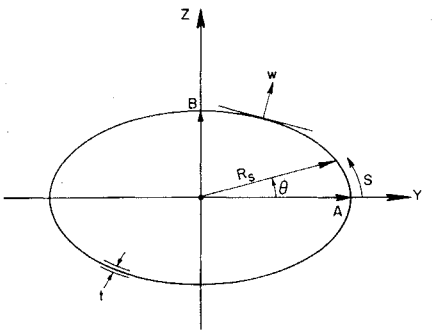

Fig. 1 Geometry of elliptical cylinders.

If the initial buckling behaviour of oval cylinders is indeed imperfection sensitive, then it is plausible, based on the aforementioned observation, that the buckling load reduction due to axial imperfection distributions can be estimated using circular cylinder axisymmetric imperfection theory appropriately modified by the curvature R_B. Although Hutchinson[3] obtained values of the postbuckling coefficient b as a function of B/A, which indicated imperfection sensitivity for oval cylinders, it was assumed in the asymptotic analysis that the initial deviation of the middle surface was in the shape of the classical buckling mode of the cylinder. Consequently, it is of interest to determine the effect of finite amplitude imperfections of various wavelengths on the buckling of elliptical cylinders by considering an imperfection profile of the form

$$\bar{W}(x) = -\mu\cos 2px/R_B \tag{5}$$

In order to estimate the load reduction due to an axial imperfection distribution given by Eq. (5), the results of Koiter's[6] axisymmetric imperfection theory for circular cylinders can be employed. The following eigenvalue equation in terms of the critical buckling load parameter λ was derived by Koiter[6] and solved[5] for arbitrary values of imperfection amplitude and wavelength:

$$A_1\lambda^3 + A_2\lambda^2 + A_3\lambda + A_4 = 0 \tag{6}$$

where

$$A_1 = -512K^6Q^2 \tag{7a}$$

$$A_2 = 64K^4Q^4 + 1024K^8 + 128K^4BQ^2 + 128c\mu\tau^2K^4Q^2 \tag{7b}$$

$$A_3 = -16K^2BQ^4 - 256K^6B - 8K^2Q^2B^2 - 16c\mu\tau^2K^2Q^2B + 512c\mu\tau^2K^6B \tag{7c}$$

$$A_4 = Q^4B^2 + 16K^4B^2 - 64c\mu\tau^2K^4B^2 + 64(c\mu)^2K^4Q^2\tau^4B^2H \tag{7d}$$

$$Q = 2K^2 + \tau^2 \tag{7e}$$

$$B = 16K^4 + 1 \tag{7f}$$

$$H = (1/Q^2) + 1/(18K^2 + \tau^2)^2 \tag{7g}$$

The results obtained from the solution of Eq. (6) can be applied to the elliptical cylinder problem by computing an equivalent circular cylinder classical axisymmetric buckling mode wave number in terms of the radius of curvature R_B at the ends of the minor axis,

$$q_o = [12(1 - \nu^2)]^{1/4}(R_B/t)^{1/2} \tag{8}$$

With this modification, it is postulated that the buckling load reduction resulting from an axial imperfection of the form of Eq. (5) can be estimated by Eq. (6) if the cylinder is sufficiently thin. A comparison of the asymptotic solution of Eq. (6) for the case when $K = \frac{1}{2}$ (i.e., the initial shape imperfection has the form of the classical axisymmetric buckling

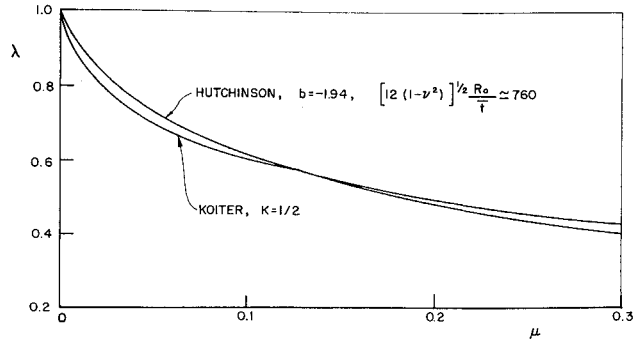

Fig. 2 Comparison of elliptical shell theory with axisymmetric imperfection circular cylinder theory for the case of $K = \frac{1}{2}$.

mode) with the results obtained by Hutchinson[3] for the elliptical cylinder can be made. In the limiting case of $\mu \to 0$ and $K = \frac{1}{2}$, Eq. (6) reduces to

$$(1 - \lambda)^2 = \tfrac{3}{2}c\mu\lambda \tag{9}$$

The corresponding asymptotic buckling load solution for the case of the elliptical cylinders is[3]

$$(1 - \lambda)^{3/2} = \tfrac{3}{2}(3)^{1/2}(-b)^{1/2}\mu\lambda \tag{10}$$

where b is a function of B/A, R_o/t, and ν. For the range of imperfect elliptical shells considered in this investigation, $0.5 \leq B/A \leq 0.8$ and $[12(1 - \nu^2)]^{1/2}R_o/t \simeq 760$. From Ref. 3, it can be shown that b is approximately constant, having an average value of -1.94. Figure 2 contains a plot of the solutions obtained for λ from both Eqs. (9) and (10) for $0 \leq \mu \leq 0.30$. In general, the agreement is quite close. Thus, it is concluded that Eqs. (6) and (8) represent valid approximations for estimating the effect of imperfection distributions of the form of Eq. (5) on the buckling behaviour of elliptical cylinders.

III. Experiment—Fabrication and Test Procedure

All test cylinders used in the experimental programe were manufactured from a liquid epoxy plastic using the spin-casting process.[7] This particular method required each cylinder to be spun-cast in a circular form. The final elliptical cross section was obtained by bonding each shell to machined aluminum end plates having the desired elliptical shape. Although both cylinder ends were contoured to the specific configuration desired, it was necessary to perform profile measurements on each cylinder by making axial traverses with two diametrically opposed, linear contacting, low-pressure displacement transducers to determine the deviations in shape from the end cross section. Particular attention was given to the proper alignment of the two-end plates with respect to the major and minor axes to prevent

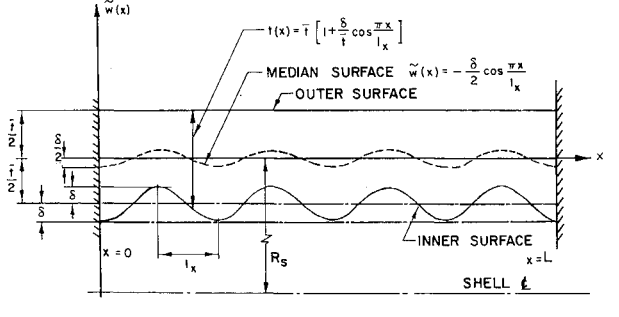

Fig. 3 Geometry of axial imperfection profile in elliptical cylinder.

Table 1 Properties of perfect elliptical cylinders and test results

$\frac{B}{A}$	$\frac{RB}{t}$	$\bar{t}$	Ex 10^5 (psi)	$\frac{\sigma c_E}{\sigma c_c}$	$\frac{\sigma cr}{\sigma c_E}$	$\frac{\sigma cr}{\sigma c_c}$	$\frac{\sigma \max}{\sigma cr}$
0.5	9.97	0.0207 ± 4%	3.84	0.386	0.815	0.317	1.19
0.6	7.89	0.0209 ± 4%	3.88	0.489	0.888	0.423	1.00
0.7	6.42	0.0247 ± 2%	4.09	0.600	0.899	0.541	1.00
0.8	5.32	0.0209 ± 4%	3.86	0.725	0.837	0.609	1.00

$\nu = 0.40$, $L = 11.0$ in., $R_o = 3.86$ in.

rotational asymmetry of the shell cross section. Thus, in each case, a circular cylinder of radius R_o was deformed into an elliptical shape for both the perfect and axially imperfect test series covering a range of eccentricity given by $0.5 \leq B/A \leq 1.0$. The edge constraint provided by each end plate corresponded to the clamped case as noted from the circular cylinder tests[5] ($B/A = 1.0$). The axial imperfection distributions given by Eq. (5) were constructed by a hydraulic tracer-tool apparatus in conjunction with a metal template containing the desired harmonic wave profile of given wavelength and amplitude.[5] This operation was performed prior to removing the spun-cast circular cylinders from the mold and resulted in an axial imperfection distribution on the inner shell surface only, as shown in Fig. 3. Tables 1 and 2 summarize the pertinent cylinder geometry for both the perfect and axially imperfect shells. Typical profiles of the median surface deviations referenced to the elliptical cross section at the shell ends for both the perfect

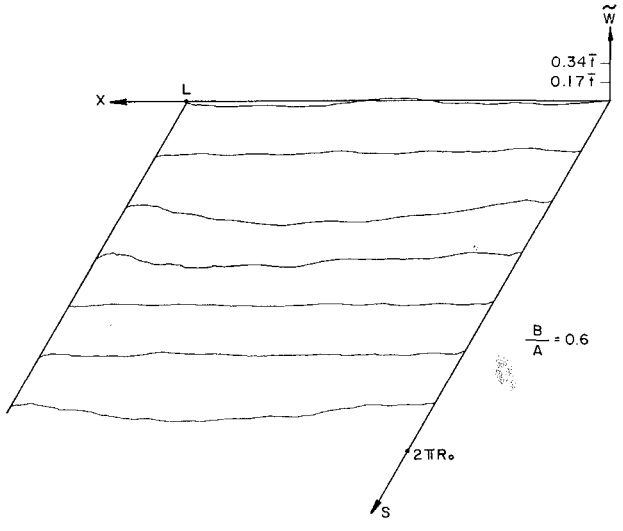

Fig. 4a Median surface profiles of the random shape imperfections present in an elliptical cylindrical shell.

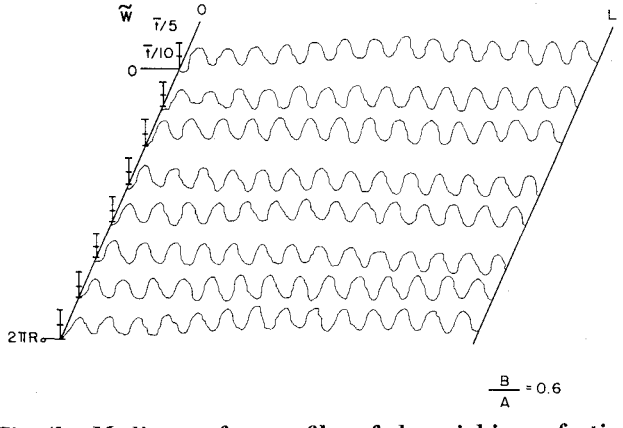

Fig. 4b Median surface profiles of the axial imperfection distribution for an elliptical cylindrical shell.

Table 2 Properties of imperfect elliptical cylinders and test results

$\frac{B}{A}$	lx in.	δ in.	$\bar{t}$ in.	$\frac{\delta}{2\bar{t}}$	K	E 10^5 (psi)	λ_K	$\frac{\sigma_{cr}^*}{\sigma_{c_E}}$	$\frac{\sigma_{\max}^*}{\sigma_{cr}^*}$
0.5	1.378	0.0021	0.0167	0.063	0.262	3.84	0.79	0.626	1.38
0.6	0.393	0.0021	0.0148	0.071	0.768	3.88	0.79	0.710	1.05
0.7	1.378	0.0021	0.0161	0.065	0.206	4.09	0.84	0.741	1.00
0.8	0.243	0.0018	0.0167	0.054	1.083	3.86	0.95	0.864	1.00

$\nu = 0.40$, $L = 11.0$ in., $R_o = 3.86$ in.

and axially imperfect cylinders are shown in Fig. 4. It is particularly significant to note that the method of fabricating the elliptical cylinders resulted in small variations from the assumed shape for the length of shells considered. However, it remains to determine the effect of the initial circumferential strains induced by the manufacturing process on the buckling behaviour of the cylinders. Hence, a series of elliptical cylinders with no specified imperfection distribution was investigated to ascertain the validity of Eq. (1) and the circular cylinder approximation. In addition, these results provided a reference basis for estimating the load reduction due to axial imperfection profiles considered in the subsequent set of tests. Initial postbuckling and maximum buckling loads were recorded for each shell to determine the extent to which cylinder eccentricity affected the postbuckling behaviour. All tests were performed in a constant end displacement, 60,000 lb, electrically driven, four-screw compression machine. In each case, initial buckling was characterized by a sudden drop in the load indicator, accompanied by a buckle pattern localized in the region of minimum curvature. The results obtained from this investigation are discussed in the next section.

IV. Discussion of Experimental Results

A comparison of the experimental buckling loads with the predicted values based on Eq. (1) for $0.5 \leq B/A \leq 1.0$ is given in Fig. 5. Assuming the clamped edge constraint accounts for a nominal 10% reduction in the buckling loads below the classical value as established by the circular cylinder tests,[8] it can be seen that the average deviation from Eq. (1) is approximately 5%. Since Eq. (1) yields results for the perfect elliptical shells considered in this program 5% lower than the exact model theory,[3] it can be concluded that on the average, the cylinders buckled within 10% of the reduced classical load, taking into account the clamped end condition. The effect of cylinder ellipticity on reducing the critical buckling load below the equivalent circular cylinder value is demonstrated in Fig. 6. In general, the agreement with the predicted response given by Eq. (2) is quite close. From the results contained in Table 1 for the perfect elliptical cylinders, it is clearly evident that the maximum support loads encountered for highly eccentric cylinders are not significantly larger than the initial buckling values. By contrast, the buckling load of an equivalent circular cylinder can be several times greater than that for an elliptical cylinder having moderate to high eccentricity. Hence, if the imperfection sensitivity of the elliptical and circular cylinders is of the same order, no design advantage can be gained by using an oval cross section as far as buckling loads are concerned.

Figure 7 contains photographs of the photoelastic isoclinic patterns corresponding to the first postbuckled equilibrium configuration for two-elliptical cylinders ($B/A = 0.5$, 0.8), as seen through a plane reflection polariscope. It is apparent that even the highly eccentric cylinder exhibits a pronounced initial buckling pattern which rapidly propagates circumferentially with increased loading.

Several imperfect elliptical cylinders were tested in axial compression to determine the load reduction resulting from axial imperfection distributions given by Eq. (5), using various values of l_x (refer to Table 2). Figure 8 shows a comparison of the experimental buckling loads for the imperfect shells [normalized by the perfect cylinder values as obtained from Eq. (1)] with the predicted results from Eqs. (6–8). It should be noted that the method of fabricating the axial imperfection profile in the elliptical cylinders resulted in an axial thickness variation which was not taken into account in the derivation of Eq. (6). However, based on the circular cylinder results previously published[5] in which an exact model formulation was used to estimate the effect

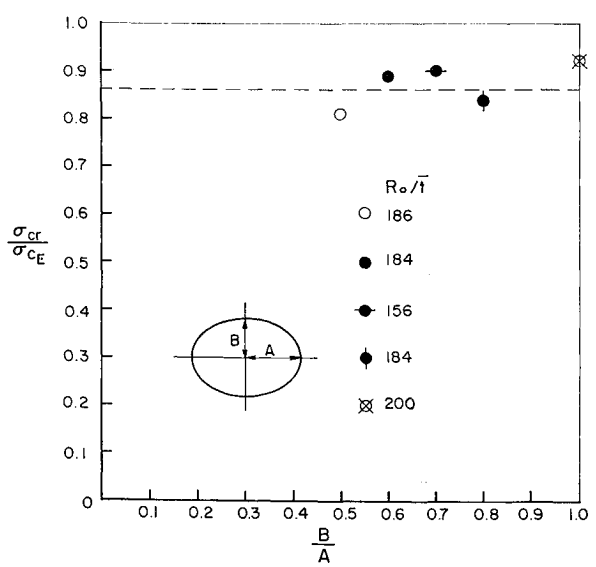

Fig. 5 A comparison of elliptical cylinder buckling loads with theory.

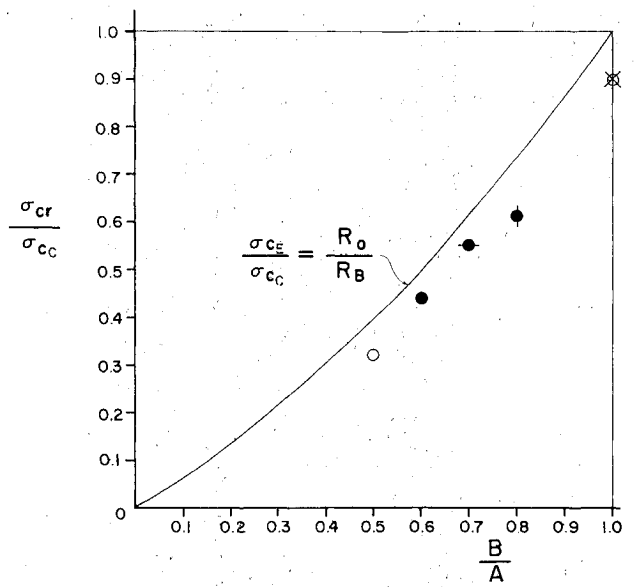

Fig. 6 Effect of cylinder ellipticity on the critical buckling load.

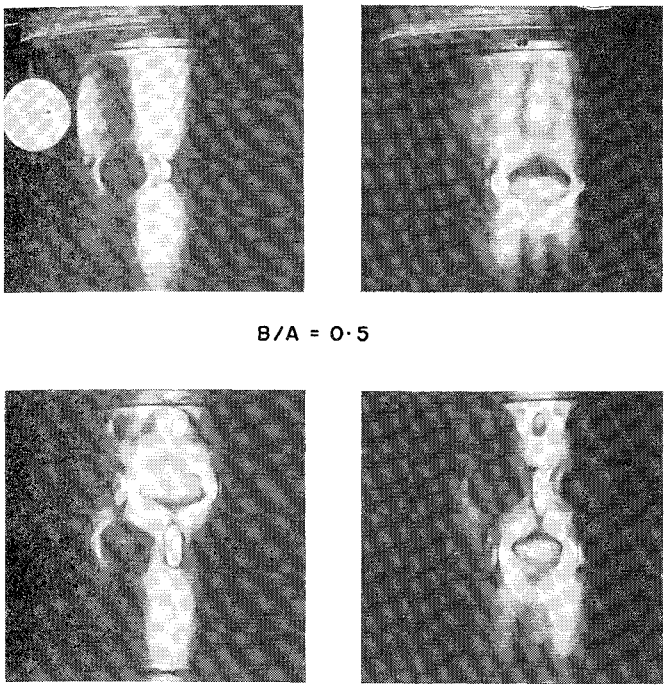

Fig. 7 Isoclinic patterns ($\theta = 45°$) corresponding to first postbuckled configuration for two elliptical cylinders.

of an axisymmetric thickness variation of the type shown in Fig. 3, it was found that the buckling load reduction was governed almost entirely by the associated initial deflection of the median surface. The difference between the buckling load solutions obtained from the application of Eq. (6) and the exact model theory amounted to nominally 2%. Consequently, it is concluded that the close agreement between experiment and theory in Fig. 8 suggests that an accurate estimate of the critical buckling load can be determined from Eq. (6), based on the radius of curvature at the ends of the minor axis. The effect of varying the axial imperfection wavelength is shown in Fig. 9, assuming an average value of the imperfection amplitude of the median surface given by $\mu = 0.063$. Again, the agreement between the predicted response and the experimental data is quite good. Hence, it is concluded that for the range of eccentricities studied, initial buckling of elliptical cylinders is indeed imperfection sensitive as predicted by Hutchinson.[3] For the type of imperfection considered, a critical wavelength exists which leads to a minimum buckling load as determined from Eq.

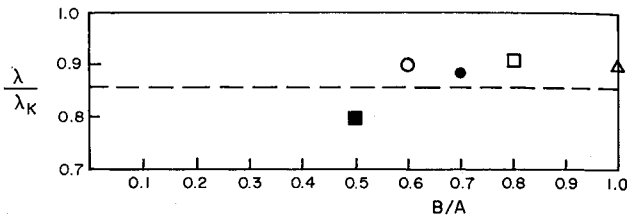

Fig. 8 Comparison of experimental buckling loads with Koiter's extended theory vs B/A.

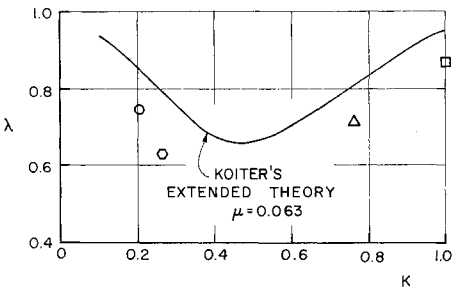

Fig. 9 Comparison of imperfect elliptical cylinder buckling loads with Koiter's extended theory for a range of axial imperfection wavelengths.

(6). It would appear that for $0.5 \leq B/A \leq 1.0$, the sensitivity of elliptical cylinders to various imperfection distributions can be accurately predicted using circular cylinder imperfection theory appropriately modified by the curvature R_B, providing the shell is sufficiently thin.

During the compression tests, plots of the applied compressive load vs cylinder end displacement were compiled to provide a measure of the postbuckling behaviour. Figure 10 contains characteristic load-displacement curves for two-elliptical cylinders to indicate the transition in postbuckling behaviour as noted by Kempner and Chen.[2,4] Although maximum compressive loads exceeding the initial buckling values were observed for large values of cylinder eccentricity, at no time did these values exceed the initial buckling load by a factor of 1.5. A summary plot illustrating the effect of cylinder eccentricity on the maximum load for both perfect and imperfect cylinders is shown in Fig. 11. Transition in postbuckling behaviour occurs for $B/A > 0.6$ and $B/A > 0.7$ for the perfect and imperfect cases, respectively.

V. Conclusions

Although the method of fabricating the elliptical cylinders used in the investigation resulted in initial strains in the

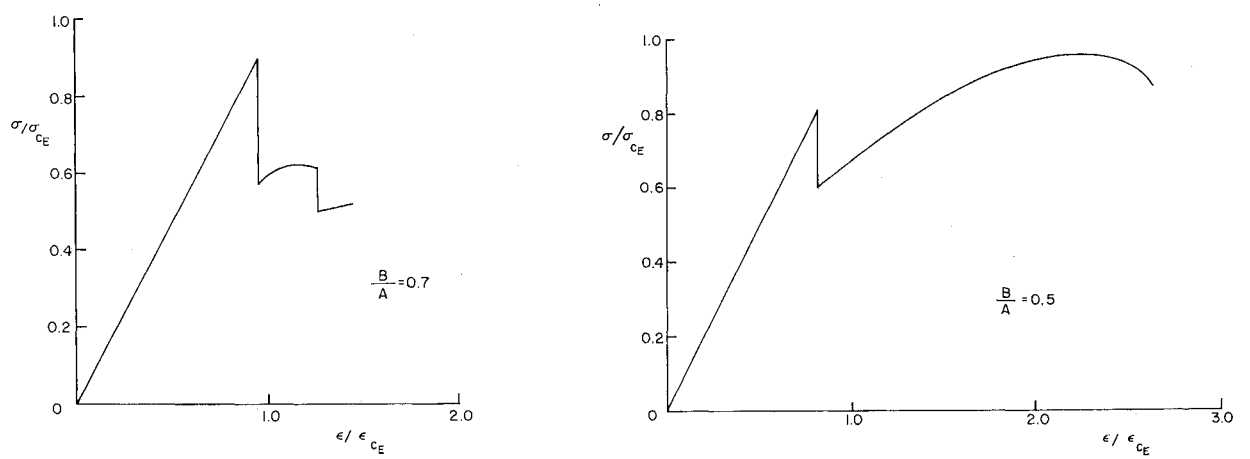

Fig. 10 Load-deflection characteristics of elliptical cylinders under axial compression.

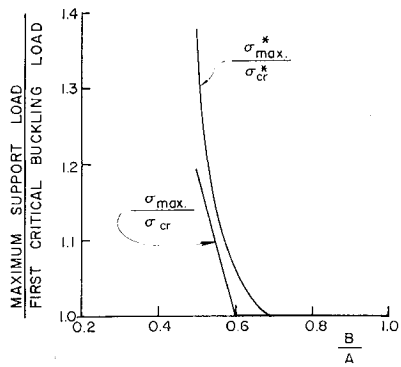

Fig. 11 Effect of eccentricity on maximum load for perfect and imperfect elliptical shells.

shell wall, it was found that the cylinders were sufficiently perfect to buckle close to the predicted classical value based on the circular cylinder equation. In addition, it was observed that significant reductions below the perfect shell buckling loads occurred for the imperfect elliptical cylinders containing small amplitude axial imperfection distributions. Using Koiter's theory for an equivalent axisymmetric imperfect circular cylinder having a radius of curvature R_B, it was shown that the imperfect elliptical cylinder buckling loads could be accurately determined. For large values of eccentricity, maximum compressive loads in excess of the initial buckling load were also noted. In general, it is concluded that elliptical cylindrical shells are indeed sensitive to small geometrical imperfections in shape as predicted by Hutchinson.

References

[1] Kempner, J., "Some Results on Buckling and Postbuckling of Cylindrical Shells," *Collected Papers on Instability of Shell Structures*, TN D-1510, Dec. 1962, NASA.

[2] Kempner, J. and Chen, Y. N., "Buckling and Postbuckling of an Axially Compressed Oval Cylindrical Shell," *Proceedings, Symposium on the Theory of Shells to Honour Lloyd Hamilton Donnell*, Univ. of Houston, McCutchan Publishing Corp., May 1967, pp. 141–183; also PIBAL Rept. 917, April 1966, Polytechnic Institute of Brooklyn.

[3] Hutchinson, J. W., "Buckling and Initial Postbuckling Behaviour of Oval Cylindrical Shells Under Axial Compression," *Transactions of the American Society of Mechanical Engineers, Journal of Applied Mechanics*, March 1968, pp. 66–72.

[4] Kempner, J. and Chen, Y. N., "Postbuckling of an Axially Compressed Oval Cylindrical Shell," *Applied Mechanics Proceedings*, 12th International Congress of Applied Mechanics, Aug. 1968, Stanford Univ.; also Springer-Verlag, New York, 1969, pp. 246–276; also PIBAL Rept. 68-31, Nov. 1968.

[5] Tennyson, R. C. and Muggeridge, D. B., "Buckling of Axisymmetric Imperfect Circular Cylindrical Shells Under Axial Compression," *AIAA Journal*, Vol. 7, No. 11, Nov. 1969, pp. 2127–2131.

[6] Koiter, W. T., "The Effect of Axisymmetric Imperfections on the Buckling of Cylindrical Shells Under Axial Compression," *Proceedings of the Royal Netherlands Academic Sciences*, Amsterdam, Series B, Vol. 66, No. 5, 1963.

[7] Tennyson, R. C., "An Experimental Investigation of the Buckling of Circular Cylindrical Shells in Axial Compression Using the Photoelastic Technique," Rept. 102, Nov. 1964, Univ. of Toronto Institute for Aerospace Studies, Toronto, Ontario, Canada.

[8] Tennyson, R. C., "Photoelastic Circular Cylinders in Axial Compression," *American Society for Testing and Materials*, STP No. 419, 1967, pp. 31–45.

FEBRUARY 1971 AIAA JOURNAL VOL. 9, NO. 2

Turbulent Boundary Layer on a Rotating Disk Calculated with an Effective Viscosity

PAUL COOPER
Case Western Reserve University, Cleveland, Ohio

The incompressible laminar and turbulent boundary-layer flow associated with a rotating disk in an infinite fluid otherwise at rest is calculated. The continuity and two boundary-layer momentum equations are solved by a method adapted from the two-dimensional finite-difference approach of Cebeci and Smith. For the outer portion of the disk where the boundary layer is turbulent, the two Reynolds stress terms involved are replaced by a two-layer scalar eddy viscosity model. Full calculation of boundary-layer development is achieved from the axis of the disk out to a radius corresponding to a rotational Reynolds number $\omega r^2/\nu$ of 10^7. The skewed velocity profiles obtained agree well with experimental data, as do also the results for boundary-layer thickness and skin-friction drag. A kind of three-dimensional turbulent boundary-layer equilibrium appears in a defect similarity of the circumferential mean turbulent velocity profiles.

Nomenclature

A_1, A_2, A_3 = geometrical coefficients in finite-difference expressions
C_M = integrated disk friction moment coefficient = $2M/(\rho\omega^2 R^5/2)$
$c_{f,\theta}$ = circumferential local skin-friction coefficient = $\tau_{w,\theta}/(\rho\omega^2 r^2/2)$
f = radial stream function
g = circumferential stream function
H = shape factor = δ^*/θ
k_1 = von Kármán's constant = 0.4

Received February 18, 1970; revision received August 3, 1970. This research was supported in part by NASA grant NGR 36-003-139. The author wishes to express his appreciation to T. Cebeci and A. M. O. Smith of the McDonnell Douglas Corporation for supplying their computer program and to Dr. Eli Reshotko of Case Western Reserve University and Werner R. Britsch of NASA for their direction and support.

* Graduate Student, Division of Fluid, Thermal and Aerospace Sciences, School of Engineering; also fluids Engineering Specialist at TRW Inc., Cleveland, Ohio.